Environmental Pollution 164 (2012) 259–266

Contents lists available at SciVerse ScienceDirect

Environmental Pollution

journal homepage: www.elsevier.com/locate/envpol

Oxidative dissolution of polymer-coated CdSe/ZnS quantum dots under UV irradiation: Mechanisms and kinetics

Yang Li [a,b], Wen Zhang [b], Kungang Li [b], Ying Yao [b], Junfeng Niu [a], Yongsheng Chen [b,*]

[a] State Key Laboratory of Water Environment Simulation, School of Environment, Beijing Normal University, Beijing 100875, PR China
[b] School of Civil and Environmental Engineering, Georgia Institute of Technology, Atlanta, GA 30332, USA

ARTICLE INFO

Article history:
Received 9 December 2011
Received in revised form
27 January 2012
Accepted 31 January 2012

Keywords:
Dissolution
QDs
UV Irradiation
ROS
Kinetics

ABSTRACT

To advance the knowledge of environmental fate of nanomaterials, we systematically investigated the dissolution of polymer-coated CdSe/ZnS quantum dots (QDs) under UV (254 nm) irradiation. The environmental effects (i.e., irradiation intensity, dissolved oxygen, temperature, and humic acid), as well as the coating effects on dissolution kinetics of QDs were investigated. Our results showed that higher irradiation intensity and temperature increased ion release rates (Cd^{2+}, SeO_4^{2-}, and Zn^{2+}), whereas the different polymer coatings varied the dissolution rates. The absence of dissolved oxygen inhibited the dissolution of QDs, and we further demonstrated that the dissolution was a photo-oxidative process involved superoxide radical formation. Humic acid had a twofold effect on dissolution due to its photosensitization and photoabsorption for UV irradiation. Finally, an empirical kinetic law was proposed to interpret the above environmental effects. This study lays groundwork to better understand the environmental fate of QDs.

1. Introduction

Semiconductor quantum dots (QDs) have been widely used in many fields such as medical diagnostics (Chen et al., 2008), drug delivery (Walther et al., 2008), DNA-based nanosensors (Zhang and Hu, 2010; Zhang et al., 2005), and solar energy conversion (Luque et al., 2007). CdSe/ZnS QDs are one of the frequently utilized QDs in these fields owing to their unique optical properties such as bright fluorescence (Michalet et al., 2005), wide absorbance range (Nga et al., 2011), narrow emission spectrum (Michalet et al., 2005), broad UV excitation (Zhang et al., 2011a), and size-dependent emission (van Sark et al., 2001).

With the rapid growth in commercial and biomedical applications, QDs may eventually enter the environment (Navarro, 2012; Slaveykova and Startchev, 2009; Zhang et al., 2007). Even after conventional water treatment, residual QDs could remain in treated water (Zhang et al., 2007). The residual QDs may undergo weathering and release toxic ions that exhibited toxicity to bacteria (Mahendra et al., 2008; Wang et al., 2011), Chlamydomonas reinhardtii (Domingos et al., 2011), and macroinvertebrate (Lee et al., 2010). Therefore, it is of great importance to understand the environmental fate and transformation such as dissolution of QDs after their entry into environment. Previous studies indicated that exposure to dissolved oxygen (DO) led to Cd^{2+} release from QDs (Derfus et al., 2004; Guo et al., 2003). Successive addition of an inorganic layer (ZnS), small organic ligands (mercaptoacetic acid), and a cross-linked organic shell (bovine serum albumin) progressively decreased the dissolution of CdSe QDs (Derfus et al., 2004). Despite many literature reported the dissolution of QDs (Cho et al., 2007; Kirchner et al., 2005; Llopis et al., 2011), the dissolution mechanisms and kinetics of QDs have not been systematically investigated yet. Moreover, the environmental effects (e.g., temperature) and the effect of different polymer surface coatings on ion release kinetics of QDs have not been well documented.

The photo-induced production of reactive oxygen species (ROS) has been attributed as one of the key mechanisms for causing instability and dissolution of QDs (Cho et al., 2007; Ipe et al., 2005; Pechstedt et al., 2010), although it is not completely unanimous about the role of ROS in photochemical dissolution. For example, CdSe/ZnS QDs stabilized with mercaptoacetic acid ligands did not produce any radicals under UV irradiation (Ipe et al., 2005). However, some studies found that $^{\bullet}OH$ was generated by CdSe/ZnS QDs under UV irradiation (Llopis et al., 2011), and $^{\bullet}OH$ and $O_2^{\bullet-}$ were both detected in illuminated CdSe/ZnS QDs with biotin surface coating (Green and Howman, 2005). Furthermore, QDs are considered as efficient energy donors that could transfer energy to O_2 to produce singlet oxygen ($^1O_2$) (Clapp et al., 2004). The ROS production not only promotes the weathering process of QDs but also has adverse biological impacts (Bakalova et al., 2004).

* Corresponding author.
E-mail address: yongsheng.chen@ce.gatech.edu (Y. Chen).

0269-7491/$ – see front matter © 2012 Elsevier Ltd. All rights reserved.
doi:10.1016/j.envpol.2012.01.047

Particularly, QDs induced ROS generation inside bacterial cells but the species of ROS were not identified (Slaveykova et al., 2009). Clearly, there is a need to understand the ROS formation mechanisms of QDs and to pinpoint the role of ROS in the photochemical stability of QDs.

This study aims to elucidate the dissolution mechanisms of QDs in aqueous environments with exposure to UV irradiation, which is generally present in natural environments and enhanced water treatment process (e.g., UV disinfection). Polydiallydimethylammounium chloride (PDDA)-coated CdSe/ZnS QDs were selected for this research because they are commercially available and representative QDs (Zimnitsky et al., 2007), which exhibit good colloidal stability. PDDA is a positively charged ionic polymer that acts as both the reducing and stabilizing agent that prevents oxidation and agglomeration (Chen et al., 2006; Yang et al., 2005). Particularly, the environmental effects (i.e., irradiation intensity, DO, temperature, and HA) and polymer coating effects on the dissolution kinetics of polymer-coated CdSe/ZnS QDs were investigated. Finally, we analyzed the formation of ROS and proposed the dissolution kinetics model equation based on the reaction stoichiometry. To the best of our knowledge, it is the first time that the environmental and coating effects on dissolution kinetics as well as the dissolution mechanism of QDs under UV irradiation are systematically investigated. Knowledge obtained from the dissolution kinetics study should also benefit the understanding of fate and transformation of QDs after their entry into the UV treatment process, where the transformation of QDs largely depends on the UV exposure conditions (e.g., irradiation intensity and exposure time).

2. Materials and methods

2.1. Materials

Water suspensions of CdSe/ZnS core/shell QDs with three types of coatings were purchased from American Ocean NanoTech, LLC. The coatings are PDDA, poly (ethylene glycol) (PEG) with a carboxylic acid terminal end group, and PEG with an amine terminal end group, respectively. The molar concentrations of the three types of QDs were 8.0 μM. The total Cd concentrations of the three types of QDs in their stock suspension were 907 ± 18, 700 ± 10, and 382 ± 14 mg/L, respectively. The dissolved Cd^{2+} concentration from the three types of QDs in their stock suspensions were also measured as 0.45 ± 0.02, 0.32 ± 0.01, and 0.19 ± 0.01 mg/L, respectively, which accounts for approximately 0.5% of the total Cd. According to the vendor, QDs will remain monodisperse in the stock solution without aggregation for one year when stored in a sealed bottle at 4 °C. Other chemicals used are shown in section S1 of the Supporting Information (SI). Deionized (DI) water (resistance >18.2 MΩ) produced by a water purification system (Thermo Scientific, USA) was used for the preparation of all solutions.

2.2. Characterization of QDs

The morphology and size of the original stock suspensions of QDs were determined by high-resolution transmission electron microscopy (HR-TEM) on a Philips EM420 at 450 kV. Each TEM sample was prepared by placing a drop of fresh aqueous QD suspension on the surface of a copper grid with a continuous carbon film coating, followed by evaporation in the dark at room temperature. The mean particle size distribution was statistically computed from at least 30 particles for each type of QDs via the image processing and analysis program ImageJ.

Hydrodynamic diameters and particle size distributions (PSDs) were determined by dynamic light scattering (DLS) on a Zetasizer Nano ZS instrument (Malvern Instruments, UK) using 1 mL of diluted aqueous QD suspension in a standard macro-cuvette (1 cm in pass length). The temperature was maintained at room temperature (25 ± 2)°C, and the scattering angle was 173°. The DI water and all solutions used for QD experiments were verified via DLS analysis to be free of particles. In addition, the same Zetasizer Nano ZS instrument was employed to measure zeta potentials of QDs. The reported average zeta potentials and standard deviations were determined from three independent measurements.

Fourier transform infrared spectroscopy (FTIR) measurements were used to confirm the composition of the surface coatings. The samples were prepared by dropcasting the QD suspension onto the fluid cell (PIKE Technologies) and then drying at room temperature. Spectra were acquired in transmission mode with the empty sample chamber as blank.

2.3. Dissolution kinetics of PDDA-coated QDs under UV irradiation

Section S2 of the SI provided a detailed experimental setup. Briefly, 5 mL of QD suspension containing 1.22 nmol/L QDs (equivalent to 140 ± 3 μg/L of Cd) was prepared by diluting the concentrated stock suspension with air-saturated DI water and placed in a polystyrene Petri dish (5 cm in diameter). The Petri dish was placed under a 4 W UVP model UVGL-25 multiband ultraviolet lamp (254 nm). The distance between the UV lamp and the Petri dish can be adjusted to vary the irradiation intensity; the powder density ranged from 0.30–1.35 mW/cm^2 as measured by a UVX radiometer (Model UVX-25, UVP Co.). A blank experiment was carried out in the dark (no light exposure) to obtain the background dissolution of QDs without UV irradiation; the background dissolution was subsequently subtracted from the concentrations of released ions under UV irradiation. All dissolution experiments were conducted at least in triplicate to confirm their reproducibility. Four mL of the QD suspension was sampled at different UV exposure times (0–18 h), and the liquid sample was filtered using Amicon Ultra-4 centrifugal ultrafilter containing porous cellulose membranes with a nominal particle size limit of 1–2 nm (Amicon Ultracel 3K, Millipore, USA) to remove solid QDs. After centrifugation for 30 min (5430R, Eppendorf, German) at 7000 × g, 3 mL of the filtrate was collected and mixed with 2 mL of trace-metal grade HNO_3 (67–70%, w/w, Fisher Scientific). The metal elements of the QD samples were analyzed using inductively coupled plasma-mass spectrometry (ICP-MS, Elan DRC II, PerkinElmer, USA) as described previously (Zhang et al., 2011a). DLS measurements were used to verify that all non-dissolved QDs were removed from the filtrate. Sections S3 and S4 in the SI describe the digestion and mass balance verification for the method of quantifying QDs with the Amicon centrifugal filter.

2.4. Environmental effects on dissolution kinetics

Irradiation intensity was varied by adjusting the distance between the UV lamp and the Petri dish, as shown in Fig. S1a. The UV irradiation intensities at different distances were measured and shown in Fig. S1b. The effect of DO was studied by comparing the dissolution of QDs in aerobic and anaerobic conditions. In the aerobic condition, as mentioned above, the Petri dish was placed in the open air, and the DI water used to prepare the diluted suspension of QDs was air-saturated with a DO concentration of approximately 7.8 mg/L. In the anaerobic condition, the DI water was purged with ultrapure N_2 for 1 h to remove DO and then was transferred to an anaerobic glove box (Coy Laboratory Products Inc., USA) containing a mixture gas of 4% H_2 and 96% CO_2 (1 atm) for diluted QD suspension preparation and UV irradiation experiments. The DO concentration in the QD suspension was measured by DO meter (Orion 083010 MD, Thermo Scientific). The DO concentration in air-saturated and deoxygenated DI water was 9.1 and <0.1 mg/L, respectively. To determine the effect of temperature on the dissolution kinetics, the experiments was performed at 0 °C (in a water bath mixed with ice), 23 °C and 37 °C in a temperature-controllable oven (VWR, USA). HA is ubiquitous in surface waters and likely affects the dissolution kinetics of QDs (Hassett, 2006). In this study, the dissolution kinetics of QDs was also carried out in the presence of HA (Suwannee River humic acid II, International Humic Substances Society) at 0–50 mg/L to represent typical surface and ground water concentration (Li et al., 2009). The ion release was monitored after addition of HA under UV irradiation of 3 h.

2.5. Effect of surface coatings

As mentioned above, three types of QDs with distinct polymer surface coatings (i.e., PDDA, PEG-carboxylic acid, and PEG-amine) were used in the dissolution kinetics under the same UV irradiation and other experimental conditions.

2.6. Measurement of ROS

t-BuOH (30 mM), L-histidine (80 mM) and superoxide dismutase (SOD) (2000 unit/L) from *Escherichia coli* were used to scavenge $^{\bullet}OH$, $^1O_2$, and $O_2^{\bullet-}$, respectively. $^{\bullet}OH$, $^1O_2$, and $O_2^{\bullet-}$ concentrations were assayed according to the method described by Cho et al. (2009). Briefly, XTT sodium salt (0.15 mM, Sigma Co.) was used as an indicator for $O_2^{\bullet-}$. The stock solution (5.25 mM) was prepared and stored for no longer than one week at 4 °C. As the photochemical reaction proceeded, 1 mL of the sample was withdrawn from the Petri dish using a syringe and injected into a quartz vial. The concentration of orange-colored formazan that formed after reaction of XTT with $O_2^{\bullet-}$ was measured using an Agilent 8453 UV–vis spectrophotometer at 450 nm. The XTT reaction in the absence of QDs was determined as a control and subtracted from the values observed in the presence of QDs.

3. Results and discussion

3.1. Characterization

HR-TEM was used to characterize the morphology and measure the size of QDs. TEM images for the three types of QDs are shown in

Fig. 1a–c with the molecular formulas of the three types of QDs shown as insets. All QDs were spherical with a relatively uniform size distribution. The diameters of PDDA-coated QDs, PEG-carboxylic acid-coated QDs, and PEG-amine-coated QDs were 3.4 ± 0.5, 3.0 ± 0.4, and 3.9 ± 0.5 nm (see Fig. S2 for the particle size distribution), respectively, which agreed with the manufacturer-reported values. Some crystal lattice of QDs could be observed as marked by the red arrow, whereas the surface coating of QDs was not visualized from these TEM images.

FTIR spectra in Fig. 1d were used to confirm the presence of the QD surface coatings. A list of vibrational attributions for the coatings of the three types of QDs is shown in Table 1. The FTIR spectrum of the coating of PDDA-coated CdSe/ZnS QDs was similar to that of the pure PDDA (Chen et al., 2006), although there were slight shifts in wavenumber. The slight shift of wavenumber compared the pure PDDA may come from interaction between PDDA and QDs, which also occurred when mixing PDDA with Au nanoparticles (Chen et al., 2006). Unfortunately, for PEG-carboylic acid or PEG-amine coated QDs, the amine and carboxylic acid groups did not elicit significant signals that could be below the detection limit of FTIR.

The DLS measurement in Fig. 1e indicated that all QDs in water suspensions had hydrodynamic size distributions of approximately 60–120 nm, which was greater than the TEM measurement because TEM measures the core particle size, whereas DLS also accounts for the size contribution from surface coatings. Moreover, DLS size is greater than TEM size could also be due to some minor aggregation or the measurement bias of the DLS technique toward large particles or aggregated clusters (e.g., the scattering intensity is proportional to d^6, where d is the diameter of the suspended particles). The polydispersivity indexes (PDIs) as a measure of the broadness of the size distribution of the PDDA-, PEG-carboxylic acid-, and PEG-amine-coated QDs were 0.123, 0.352, and 0.356, respectively. When PDIs are less than 0.25, the QD suspensions are considered monodisperse without aggregation (Gutierrez et al., 2010; Zhang et al., 2011b). The number-averaged and volume-averaged PSDs are also provided in section S6 of the SI.

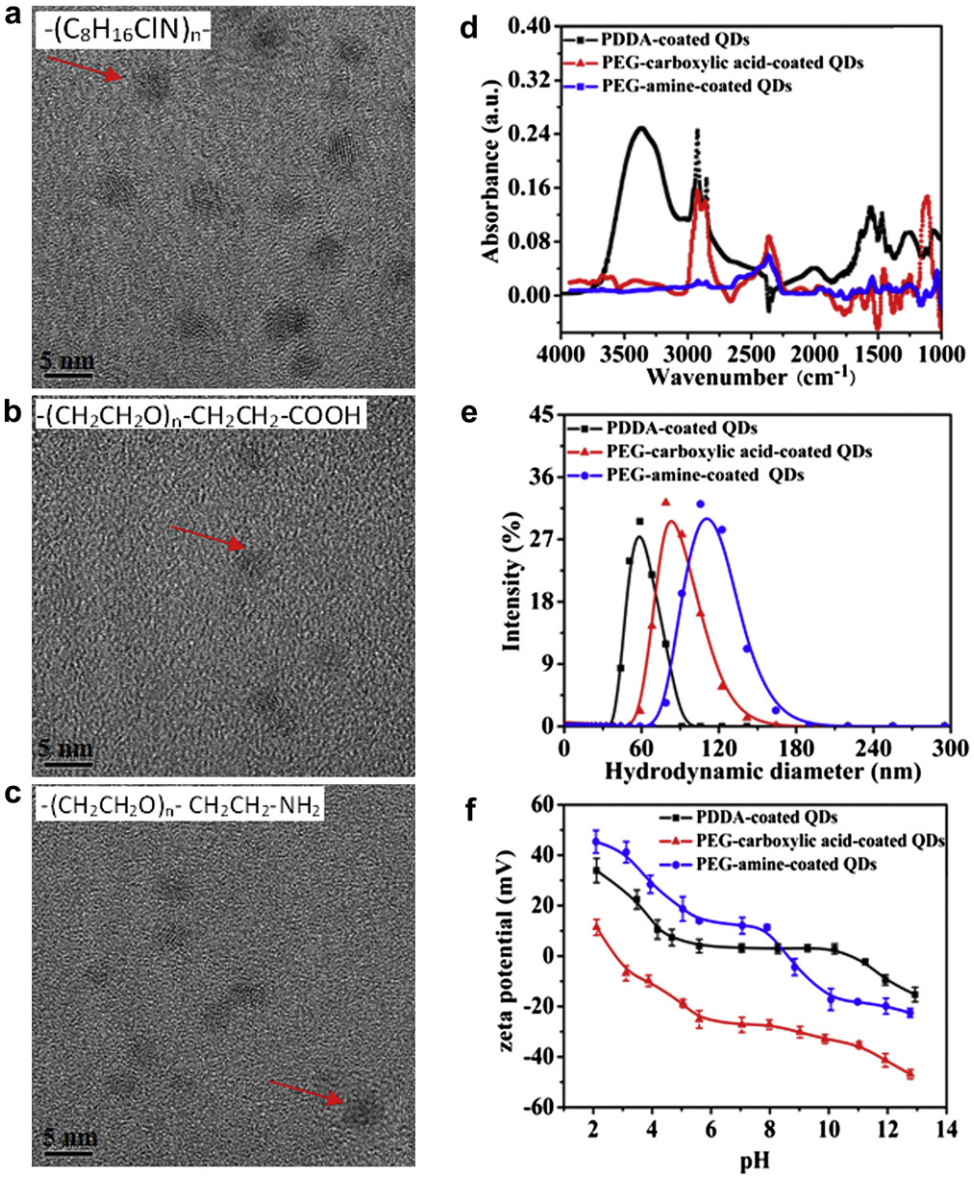

Fig. 1. (a)–(c) HR-TEM images of PDDA-, PEG-carboxylic acid-, and PEG-amine-coated QDs, (d) FTIR spectra, (e) Intensity-averaged PSD diagrams, and (f) zeta-potentials as a function of pH for the three types of QDs.

Table 1
Vibrational attributions for the coatings of the three types of QDs.

CdSe/ZnS QDs	Wavenumber (cm^{-1})	Attributions	Reference
PDDA-coated QDs	3361	O–H	(Chen et al., 2006)
	1468, 1630	$\delta_{C=C}$	
	1564	C–N	
	2923	Asymmetric CH_2	(Gregoriou
	2852	Symmetric CH_2	et al., 1997)
PEG-carboylic acid or PEG-amine coated QDs	1760	C=O	(Kolhe and Kannan, 2003)
	1110	C–O–C	(Billingham et al., 1997)
	2850–3000	CH_2	(Kolhe and Kannan, 2003)
	3200–3600	O–H	(Mansur et al., 2004)

Zeta-potentials for the three types of QDs are shown in Fig. 1f as a function of pH. At pH of 5.6 (the initial pH of our dissolution experiment), the mean zeta-potentials were 4.0, −25.2, and 14.0 mV for PDDA-, PEG-carboxylic acid-, and PEG-amine-coated QDs, respectively. The iso-electric points (pH_{zpc}) for the three types of QDs were approximately at 10.8, 2.8, and 8.7, respectively. During the zeta potential measurement, hydrodynamic diameters were also measured and the results confirmed that the QDs had no aggregation.

3.2. Effect of irradiation intensity on the dissolution kinetics of PDDA-coated QDs

As shown in Fig. 2, dissolution rates for both Cd and Se significantly increased as the irradiation intensity increased although QDs can also dissolve slightly under dark conditions. This indicates that the dissolution of PDDA-coated QDs was a photo-oxidation process as suggested previously (Ma et al., 2006; van Sark et al., 2001). While Se release was shown to increase proportionally with the increasing irradiation intensity, the release of Cd did not increase significantly as the intensity was elevated from 0.75 to 1.35 mW/cm^2. Moreover, the release of Cd reached equilibrium after approximate 5 h exposure to UV, whereas for Se the equilibrium time was approximately 12 h. The appearance of the dissolution equilibrium is clearly indicative of the presence of other limiting factors for the photo-oxidation of QDs, which is further discussed in the following mechanism section.

It is also worth mentioning that the dissolution kinetics in this study was only described by the dissolution of Cd and Se, because the released Zn^{2+} concentrations (results not shown) had certain fluctuations, probably due to chelation between the released Zn^{2+} and the PDDA molecules or the precipitation of ZnS.

3.3. Effect of DO on the dissolution kinetics of PDDA-coated QDs

Fig. 3 shows the dissolution of QDs with and without exposure to air. Within the three-hour UV irradiation, the released concentrations of Cd and Se were 50.4 and 6.8 μg/L, respectively, in the air-saturated water suspension, whereas in the glove box the released concentrations of Cd and Se were only 12.1 and 2.3 μg/L, respectively. Because of the lack of oxygen in the anaerobic glove box, the dissolution of QDs was not sustained after depletion of residual dissolved oxygen, indicating that the dissolution of QDs can only be initiated by the photo-oxidation under UV irradiation. This result agrees with the previous findings that preventing QDs from exposure to oxidative environments could inhibit Cd^{2+} release (Derfus et al., 2004; Guo et al., 2003).

3.4. Effect of temperature on the dissolution kinetics of PDDA-coated QDs

Fig. 4 shows that the temperature influence on dissolution kinetics was evident. Increasing the solution temperature from 0 to 37 °C significantly increased the release rates of both Cd and Se. Increasing temperature generally enhances the mass transfer rates of dissolved oxygen to the reaction sites on the surfaces of QDs, and also lowers the reaction activation energy, which leads to faster reaction kinetics according to the transition state theory. Thus, the effect of temperature on dissolution kinetics of QDs can also be interpreted using the Arrhenius-based kinetics model in our previous article (Zhang et al., 2011b). In this regard, the Arrhenius-based kinetics equation was employed to fit our experimental data for Cd and Se in Fig. 4 and the fit equations, correlation coefficients (R^2), as well as the fitting parameters are shown in section S7 in SI.

3.5. Effect of HA on the dissolution kinetics of PDDA-coated QDs

HA are commonly present in surface and ground water (Li et al., 2009), which may influence the environmental transformations of QDs. Fig. 5 shows that PDDA-coated QDs released more Cd and Se as the HA concentration increased from 0 to 20 mg/L and 5 mg/L, respectively, which could be the sensitization effect of HA and the generation of ROS that enhances the photo-oxidative dissolution of QDs (Fisher et al., 2006). Further increasing the concentration of HA to 50 mg/L reduced the extent of Cd release and this is probably because HA could complex with heavy metals (Kamei-Ishikawa et al., 2008; Mantoura et al., 1978; Pinheiro et al., 1994), thereby reducing the concentrations of the dissolved metal ions from QDs. Moreover, HA may act as a reducing buffer and UV filter for QDs (Vione et al., 2009) that may consume ROS and consequently inhibit the dissolution of QDs as we observed at elevating concentrations of HA.

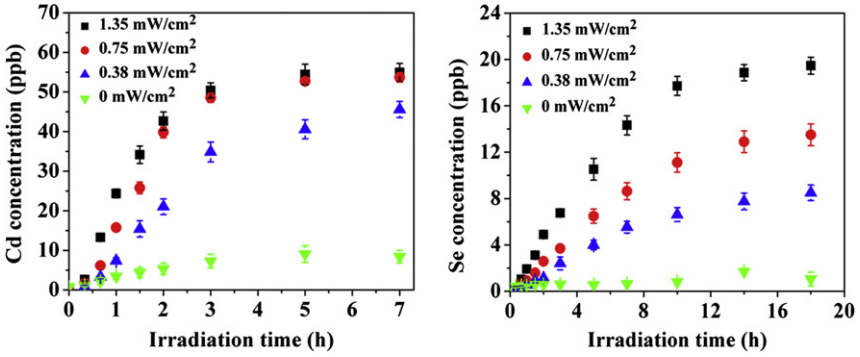

Fig. 2. Dissolution kinetics of PDDA-coated QDs in air-saturated DI water at room temperature under UV intensities of 1.35, 0.75, and 0.38 mW/cm^2 (initial pH 5.6 and initial concentration of QDs 140 ± 3 μg-Cd/L).

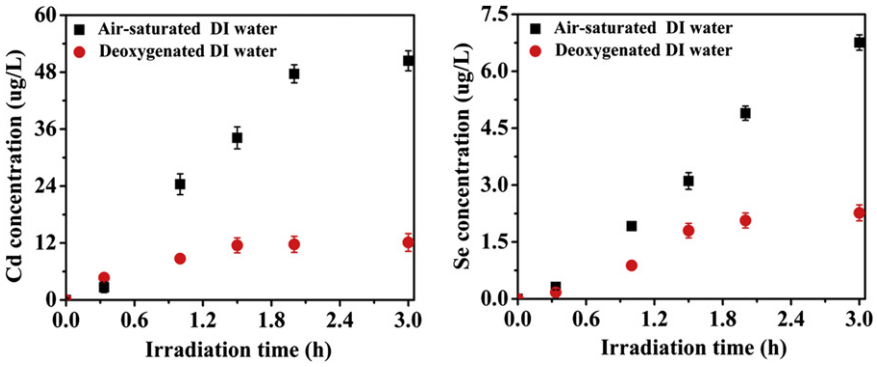

Fig. 3. Dissolution kinetics of PDDA-coated QDs in air-saturated and deoxygenated water in the glove box at room temperature under UV irradiation (UV intensity 1.35 mW/cm^2; other conditions were the same as in Fig. 2).

3.6. Effect of coatings on the dissolution kinetics of PDDA-coated QDs

Fig. 6 shows that the dissolution rate was highest for PEG-carboxylic acid-coated QDs, followed closely by PEG-amine-coated QDs, and then PDDA-coated QDs. Thus, PDDA coating appeared to resist photo-oxidation to a greater extent than PEG coating. The different dissolution rates were largely caused by the difference of the distinct surface coating molecules (Zook et al., 2011). It was reported that the QDs coated with longer chain, higher molecular weight, and structural complexity of the ligands should be more stable (Aldana et al., 2001). The chain length and structural complexity of PDDA are clearly higher than that of PEG, which probably interprets the lower dissolution rate of PDDA-coated QDs compared with those of PEG-coated QDs. Clearly, the three types of surface coatings did not prevent the photo-oxidation but only slightly inhibited the dissolution to some extents, which is consistent with previous findings (Cho et al., 2007; Derfus et al., 2004; Ma et al., 2007; van Sark et al., 2001). For example, different surface coatings (e.g., ZnS, BSA, DHLA, and polyacrylate/streptavidin) of CdSe QDs were found to affect the dissolution kinetics to different extent (Derfus et al., 2004).

Other environmental effects such as pH will certainly influence the dissolution kinetics of QDs (Schmidt and Vogelsberger, 2006; Zhang et al., 2011c). Because pH not only influences the reaction thermodynamics (see the photo-oxidation mechanism analysis below) but also changes the stability or aggregation state of QD dispersions, which also affect the dissolution kinetics (Petosa et al., 2010), it would be less meaningful to discuss the single pH effect on the dissolution kinetics. However, to investigate the dissolution mechanisms, we monitored the solution pH, which decreased slightly from 5.6 to 4.5 as the photo-oxidation reaction proceeded (see details in section S8). With the decreasing pH, the surface of QDs would be more positively charged (Fig. 1(f)), which tends to increase the electrostatic repulsion between individual QDs and leads to more stable dispersions of QDs. This is desirable because the same particle surface areas of QDs are expected to be exposed to UV irradiation so that the potential effect from the instability of QDs on dissolution kinetics was minimal.

3.7. Photo-oxidation mechanism

When QDs are excited by incident photons carrying higher energies than the band gap of QDs, a bound electron-hole pair is formed, which could react with the surrounding oxygen molecules to produce ROS, including $^1O_2$, $^{\bullet}OH$, and $O_2^{\bullet-}$ (Ipe et al., 2005; Ma et al., 2007). Two independent methods, scavenging experiments and UV–vis were conducted to analyze the formation of ROS during the dissolution of QDs under UV irradiation. The effect of radical scavengers on Cd^{2+} release kinetics is shown in Fig. 7(a). When excess $^{\bullet}OH$ (30 mM t-BuOH) and $^1O_2$ (80 mM L-histidine) scavengers were used, Cd^{2+} release did not change appreciably, indicating that $^{\bullet}OH$ and $^1O_2$ were not the main ROS involved. When excess $O_2^{\bullet-}$ scavenger (2000 unit/L SOD) was added before 90 min of reaction, a pronounced retardation of the Cd^{2+} release rate of QDs was observed, indicating that photoexcitation of QDs leads to $O_2^{\bullet-}$, which may act as a precursor inducing the oxidative dissolution of QDs. Interestingly, SOD led to an increase in Cd^{2+} release after irradiation for 90 min, probably because SOD catalyzed the conversion of $O_2^{\bullet-}$ into H_2O_2, which promoted Cd^{2+} release, as shown in the reaction below (Lovric et al., 2005):

$$2O_2^{\bullet-} + 2H_2O \overset{SOD}{\rightleftarrows} O_2 + H_2O_2 + 2OH^-$$

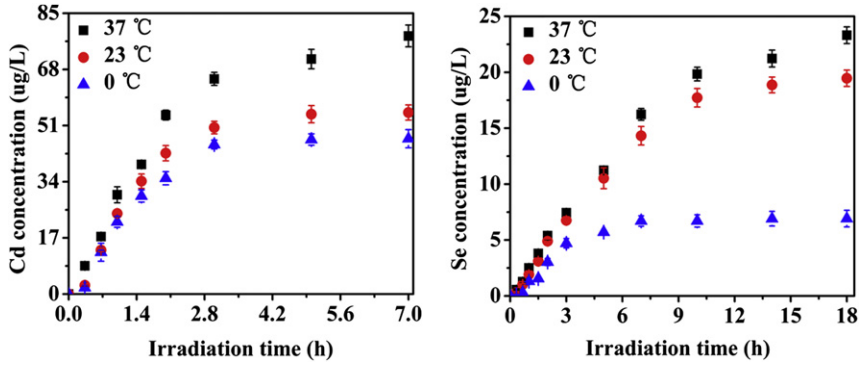

Fig. 4. Dissolution kinetics of PDDA-coated QDs in air-saturated DI water at different temperatures under UV irradiation (initial pH 5.6, initial concentration of QDs 140 ± 3 μg-Cd/L, and UV intensity 1.35 mW/cm^2).

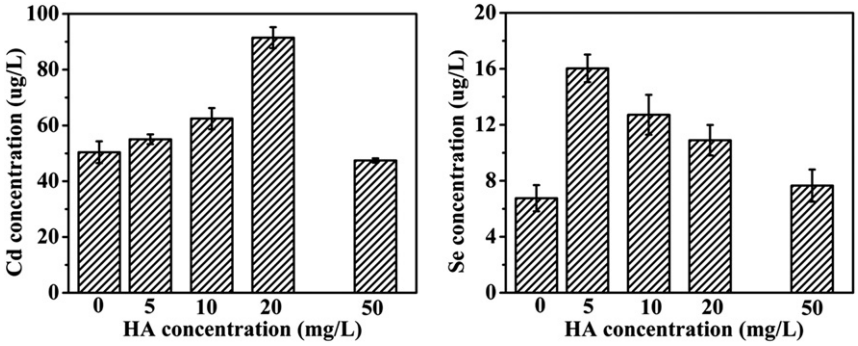

Fig. 5. Ion release of PDDA-coated QDs as a function of HA concentration after three-hour UV irradiation (initial pH 5.6, initial concentration of QDs 140 ± 3 μg-Cd/L, and UV intensity 1.35 mW/cm^2).

Thus, H_2O_2 is most likely the intermediate oxidant that reacts rapidly with QDs at ambient conditions (Pechstedt et al., 2010).

To confirm the generation of ROS, XTT was used as an indicator to investigate $O_2^{\cdot-}$. Fig. 7(b) shows the changes in the absorption spectra at $\lambda = 450$ nm that indicate the production of $O_2^{\cdot-}$. The quantity of $O_2^{\cdot-}$ produced was calculated using the molar extinction coefficient $2.16 \times 10^4\ M^{-1}\,cm^{-1}$ for XTT (Sutherland and Learmonth, 1997). The absorbance at 180 min was approximately 0.71, and thus the QDs generated $O_2^{\cdot-}$ at an estimated concentration of approximately 33.1 μM after 180 min of UV irradiation; the production rate of $O_2^{\cdot-}$ was 0.18 μM/min.

To explore the reaction stoichiometry of QDs, we first determined the possible ionic species that were present after photo-oxidation of QDs (see details in section S8). According to the E_h-pH diagrams, Cd^{2+}, SeO_4^{2-}, Zn^{2+}, and SO_4^{2-} may be the dominant aqueous species of Cd, Se, Zn, and S when pH is within 4.5–5.6 (Takeno, 2005). As mentioned above, the photo-oxidation is a proton-generating process, as supported by the observed decrease in pH. Thus, the following reaction stoichiometry was proposed for simple water chemistries:

$$Cd_{5.68}SeZn_{4.1}S_x + (x - 8.78)H_2O + (1.5x + 6.39)O_2 \overset{UV}{\rightleftarrows} 5.68Cd^{2+} + SeO_4^{2-} + 4.1Zn^{2+} + xSO_4^{2-} + (2x - 17.56)H^+$$

The above chemical formula of PDDA-coated QDs was estimated on the basis of the total element composition measurement with ICP-MS (see details in section S3). As illustrated in Fig. S6, the photo-degradation products (Cd^{2+}, SeO_4^{2-}, and Zn^{2+}) may diffuse out of the core-shell structure, resulting in the reduction of the hydrodynamic sizes of QDs as observed by DLS (see Fig. S6). Moreover, the reduction in particle size may also be resulted from the solution pH changes as indicated above. As the solution pH decreased and the interparticle repulsion from the electrostatic force was increased, which could prevent QDs from aggregation and lead to a shift in the hydrodynamic size distribution. More discussions about the change of particles size of QDs during UV irradiation was provided in section S10.

3.8. Reaction kinetics analysis

On the basis of the reaction stoichiometry, the dissolution of QDs may follow first-order kinetics, and the rate of Cd^{2+} release is expressed as:

$$r_{Cd^{2+}} = \frac{d[Cd^{2+}]}{dt} = k_{Cd^{2+}}[Cd_{5.68}SeZn_{4.1}S_x][O_2]^{1.5x+6.39} = k_{Cd^{2+}}\left\{M_0 - \frac{[Cd^{2+}]}{5.68}\right\}[O_2]^{1.5x+6.39} \quad (1)$$

where $r_{Cd^{2+}}$ is the release rate of Cd^{2+} (mol/(L h)), $k_{Cd^{2+}}$ is the reaction rate constant (mol/h), $[Cd^{2+}]$, $[Cd_{5.68}SeZn_{4.1}S_x]$, and $[O_2]$ are the molar concentrations (mol/L) of released Cd^{2+}, the QD core, and DO, respectively; and M_0 is the molar concentration (mol/L) of the original QDs before UV irradiation. Here we can define the pseudo-first-order rate constant (h^{-1}), $k_{obs}^{Cd} = k_{Cd^{2+}}[O_2]^{1.5x+6.39}$, where $[O_2]$ was found to be constant over time. Rearranging Eq. (1), the Cd^{2+} release rate can be expressed as:

$$r_{Cd^{2+}} = \frac{d[Cd^{2+}]}{dt} = k_{obs}^{Cd}\left(M_0 - \frac{[Cd^{2+}]}{5.68}\right) \quad (2)$$

Integration of Eq. (2) yields:

$$-5.68\ln\left(M_0 - \frac{[Cd^{2+}]}{5.68}\right) = k_{obs}^{Cd}t + A \quad (3)$$

where $A = -5.68\ln M_0$ because when t is zero, $[Cd^{2+}]_{released}$ is zero. Likewise, the dissolution kinetic equation for Se release can also be derived similarly. The kinetic Eqs. (1)–(3) are actually developed for

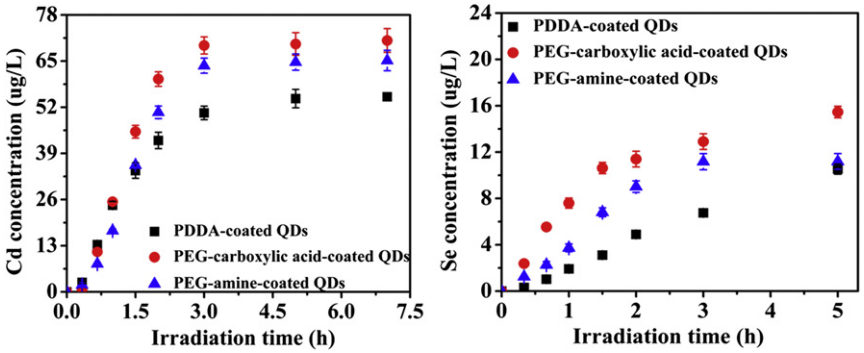

Fig. 6. Dissolution kinetics of three types of QDs in air-saturated DI water (initial pH 5.6, initial concentration of QDs 140 ± 3 μg-Cd/L, and UV intensity 1.35 mW/cm^2).

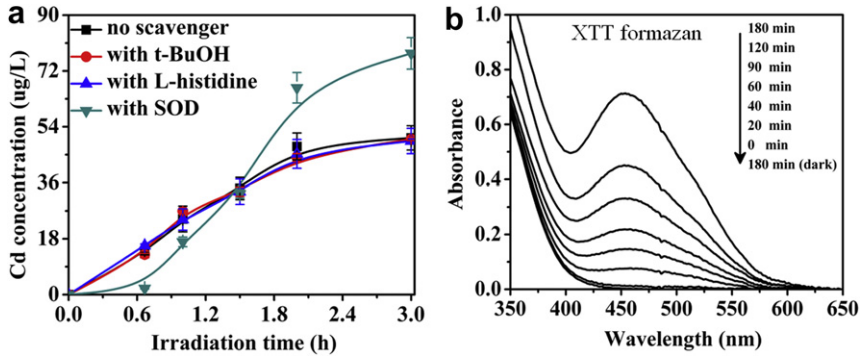

Fig. 7. (a) Dissolution kinetics of PDDA-coated QDs in the presence and absence of scavengers (initial concentration of QDs 140 ± 3 μg-Cd/L, t-BuOH 30 mM, L-histidine 80 mM, and SOD 2000 unit/L), (b) UV–Vis absorption spectra of PDDA-coated QDs in the presence of XTT as a function of irradiation time (initial concentration of QDs 1.4 ± 0.03 mg-Cd/L and XTT 0.15 mM).

ideal homogeneous reactants (e.g., molecules or ions). However, QDs exhibited particle-like heterogeneous properties. From Figs. 2–6, we can easily observe that QDs were not completely dissolved in all cases as similarly observed for the dissolution of Ag nanoparticles (Kittler et al., 2010; Zhang et al., 2011b). The degree of dissolution for nanoparticles depended on the total surface areas available for reactions and the mass transfer of electron acceptor to the available surfaces. The complete dissolution of QDs should be theoretically possible with sufficient oxygen supply and infinite reaction time. The observed equilibrium clearly does not correspond to the real physicochemical "equilibrium". The released ions accumulated on the surface and may block the oxygen transfer to the core of QDs, resulting in the quasi-equilibrium due to the lack of available surface area for oxidation. In other words, in the realistic dissolution process (e.g., no aeration or hydrodynamic disturbance), the final quasi-equilibrated concentrations of Cd or Se we observed would be less than the total Cd or Se concentrations of QDs. Thus, M_0 in the kinetic Eqs. (1)–(3) is not the total molar concentration of QDs when quasi-equilibrium occurred. To determine the actual M_0, we treated M_0 and k_{obs} as the fitting parameters and fitted the experimental data in Figs. 2, 4, and 6 using Eq. (3). Figs. S8–S10 compares the fitting curves and the experimental results, which well agreed with each other. Tables S4 and S5 summarize the correlation coefficients (R^2) and fitted values of rate constants and M_0. R^2 ranged from 0.96 to 0.99, indicating that the kinetic model in Eqs. (1)–(3) could explain at least 96% of the variance of the experimental data. Apparently, the irradiation intensity, temperature, and surface coating all influenced the magnitude of k_{obs}^{Cd} and k_{obs}^{Se}. The increasing irradiation intensity increased both k_{obs}^{Cd} and k_{obs}^{Se}, while had a minor effect on M_0. This might be reasonable because increasing irradiation intensity will increase the ROS formation and thus the oxidation rate. However, irradiation intensity does not affect the surface areas of QDs and thus exerts no effects on M_0. Regarding the surface coating effect, k_{obs}^{Cd} and k_{obs}^{Se} were highest for PDDA-coated QDs, followed by PEG-carboxylic acid-coated and PEG-amine-coated QDs. Overall, the kinetic equation in Eq. (3) was well fitted to the experimental data under various conditions; particularly, the fitted values of M_0 were less than the total molar concentration of QDs (i.e., 140 μg-Cd/L or 1.2 μmol-Cd/L), which supported our previous assumption.

4. Conclusions

An understanding of the environmental fate and transformation of QDs is needed to establish a thorough evaluation of the potential environmental and ecological risks of its emerging applications. Although the number of studies examining the weathering process of QDs is considerable, our knowledge on the mechanisms and dissolution kinetics is limited. To this end, the data reported in this study begins to fill the knowledge gaps regarding the mechanisms and kinetics of dissolution of QDs. The results suggest that the dissolution mechanism of polymer-coated QDs under UV irradiation was driven by the photo-oxidation that involves the formation of $O_2^{\cdot-}$. The dissolution kinetics of QDs is first order with respect to [QDs] and is affected by various environment factors (i.e., irradiation intensity, DO, temperature, and HA), and surface coatings. Although relatively simple water chemistries were used to facilitate the dissolution experiments and mechanism analysis, this study provide a certain insight into the potential fate and the aqueous reaction mechanisms in the presence of UV irradiation, which is not only naturally present in the environment but also used as a water purification method. Our study also implies that when QDs enter the UV treatment process, they could either totally dissolve into ions or survive as particles depending on the UV exposure conditions (e.g., irradiation intensity and exposure time). Thus, to improve the removal efficiency of QDs, knowledge of the dissolution kinetics is imperative.

Acknowledgments

This study was partially supported by the U.S. Environmental Protection Agency Science to Achieve Results Program Grant RD-83385601 and Engineering Research Center (ERC)/Semiconductor Research Corporation (SRC)/ESH grant (425.025). The first and second authors contributed equally to this work.

Appendix. Supplementary material

Supplementary material associated with this article can be found, in the online version, at doi:10.1016/j.envpol.2012.01.047

References

Aldana, J., Wang, Y.A., Peng, X., 2001. Photochemical instability of CdSe nanocrystals coated by hydrophilic thiols. Journal of the American Chemical Society 123, 8844–8850.
Bakalova, R., Ohba, H., Zhelev, Z., Ishikawa, M., Baba, Y., 2004. Quantum dots as photosensitizers? Nature 22, 1360–1361.
Billingham, J., Breen, C., Yarwood, J., 1997. Adsorption of polyamine, polyacrylic acid and polyethylene glycol on montmorillonite: An in situ study using ATR-FTIR. Vibrational Spectroscopy 14, 19–34.
Chen, H., Wang, Y., Dong, S., Wang, E., 2006. One-step preparation and ch aracterization of PDDA-protected gold nanoparticles. Polymer 47, 763–766.
Chen, L.D., Liu, J., Yu, X.F., He, M., Pei, X.F., Tang, Z.Y., Wang, Q.Q., Pang, D.W., Li, Y., 2008. The biocompatibility of quantum dot probes used for the targeted imaging of hepatocellular carcinoma metastasis. Biomaterials 29, 4170–4176.

Cho, M., Fortner, J.D., Hughes, J.B., Kim, J.H., 2009. *Escherichia coli* inactivation by water-soluble, ozonated C60 derivative: Kinetics and mechanisms. Environmental Science & Technology 43, 7410–7415.
Cho, S.J., Maysinger, D., Jain, M., Röder, B., Hackbarth, S., Winnik, F.M., 2007. Long-term exposure to CdTe quantum dots causes functional impairments in live cells. Langmuir 23, 1974–1980.
Clapp, A.R., Medintz, I.L., Mauro, J.M., Fisher, B.R., Bawendi, M.G., Mattoussi, H., 2004. Fluorescence resonance energy transfer between quantum dot donors and dye-labeled protein acceptors. Journal of the American Chemical Society 126, 301–310.
Derfus, A.M., Chan, W.C.W., Bhatia, S.N., 2004. Probing the cytotoxicity of semiconductor quantum dots. Nano Letters 4, 11–18.
Domingos, R.F., Simon, D.F., Hauser, C., Wilkinson, K.J., 2011. Bioaccumulation and effects of CdTe/CdS quantum dots on *Chlamydomonas reinhardtii* – nanoparticles or the free ions? Environmental Science & Technology 45, 7664–7669.
Fisher, J., Reese, J., Pellechia, P., Moeller, P., Ferry, J., 2006. Role of Fe (III), phosphate, dissolved organic matter, and nitrate during the photodegradation of domoic acid in the marine environment. Environmental Science & Technology 40, 2200–2205.
Green, M., Howman, E., 2005. Semiconductor quantum dots and free radical induced DNA nicking. Chemical Communications, 121–123.
Gregoriou, V.G., Hapanowicz, R., Clark, S., Hammond, P.T., 1997. Infrared studies of novel optically responsive materials: orientation characteristics of sulfonated polystyrene/poly (diallyldimethylammonium chloride) ionic polymer multilayers on patterned self-assembled monolayers. Applied Spectroscopy 51, 470–476.
Guo, W., Li, J.J., Wang, Y.A., Peng, X., 2003. Luminescent CdSe/CdS core/shell nanocrystals in dendron boxes: superior chemical, photochemical and thermal stability. Journal of the American Chemical Society 125, 3901–3909.
Gutierrez, L., Mylon, S.E., Nash, B., Nguyen, T.H., 2010. Deposition and aggregation kinetics of rotavirus in divalent cation solutions. Environmental Science & Technology 44, 4552–4557.
Hassett, J.P., 2006. Dissolved natural organic matter as a microreactor. Science 311, 1723–1724.
Ipe, B.I., Lehnig, M., Niemeyer, C.M., 2005. On the generation of free radical species from quantum dots. Small 1, 706–709.
Kamei-Ishikawa, N., Nakamaru, Y., Tagami, K., Uchida, S., 2008. Sorption behavior of selenium on humic acid under increasing selenium concentration or increasing solid/liquid ratio. Journal of Environmental Radioactivity 99, 993–1002.
Kirchner, C., Liedl, T., Kudera, S., Pellegrino, T., Javier, A.M., Gaub, H.E., St Izle, S., Fertig, N., Parak, W.J., 2005. Cytotoxicity of colloidal CdSe and CdSe/ZnS nanoparticles. Nano Letters 5, 331–338.
Kittler, S., Greulich, C., Diendorf, J., Koller, M., Epple, M., 2010. Toxicity of silver nanoparticles increases during storage because of slow dissolution under release of silver ions. Chemistry of Materials 22, 4548–4554.
Kolhe, P., Kannan, R.M., 2003. Improvement in ductility of chitosan through blending and copolymerization with PEG: FTIR investigation of molecular interactions. Biomacromolecules 4, 173–180.
Lee, J., Ji, K., Kim, J., Park, C., Lim, K.H., Yoon, T.H., Choi, K., 2010. Acute toxicity of two CdSe/ZnSe quantum dots with different surface coating in *Daphnia magna* under various light conditions. Environmental Toxicology 25, 593–600.
Li, Q., Xie, B., Hwang, Y.S., Xu, Y., 2009. Kinetics of C60 fullerene dispersion in water enhanced by natural organic matter and sunlight. Environmental Science & Technology 43, 3574–3579.
Llopis, M.V., Rodríguez, J.C.C., Martín, F.J.F., Coto, A.M., Fernández-Argüelles, M.T., Costa-Fernández, J.M., Sanz-Medel, A., 2011. Dynamic analysis of the photoenhancement process of colloidal quantum dots with different surface modifications. Nanotechnology 22, 385703.
Lovric, J., Cho, S.J., Winnik, F.M., Maysinger, D., 2005. Unmodified cadmium telluride quantum dots induce reactive oxygen species formation leading to multiple organelle damage and cell death. Chemistry & Biology 12, 1227–1234.
Luque, A., Martí, A., Nozik, A.J., 2007. Solar cells based on quantum dots: multiple exciton generation and intermediate bands. Mrs Bulletin 32, 236–241.
Ma, J., Chen, J.Y., Guo, J., Wang, C.C., Yang, W.L., Xu, L., Wang, P.N., 2006. Photostability of thiol-capped CdTe quantum dots in living cells: the effect of photooxidation. Nanotechnology 17, 2083–2089.
Ma, J., Chen, J.Y., Zhang, Y., Wang, P.N., Guo, J., Yang, W.L., Wang, C.C., 2007. Photochemical instability of thiol-capped CdTe quantum dots in aqueous solution and living cells: process and mechanism. Journal of Physical Chemistry B 111, 12012–12016.
Mahendra, S., Zhu, H., Colvin, V.L., Alvarez, P.J., 2008. Quantum dot weathering results in microbial toxicity. Environmental Science & Technology 42, 9424–9430.
Mansur, H.S., Oréfice, R.L., Mansur, A.A.P., 2004. Characterization of poly (vinyl alcohol)/poly (ethylene glycol) hydrogels and PVA-derived hybrids by small-angle X-ray scattering and FTIR spectroscopy. Polymer 45, 7193–7202.
Mantoura, R.F.C., Dickson, A., Riley, J.P., 1978. The complexation of metals with humic materials in natural waters. Estuarine and Coastal Marine Science 6, 387–408.
Michalet, X., Pinaud, F.F., Bentolila, L.A., Tsay, J.M., Doose, S., Li, J.J., Sundaresan, G., Wu, A.M., Gambhir, S.S., Weiss, S., 2005. Quantum dots for live cells, in vivo imaging, and diagnostics. Science 307, 538–544.
Navarro, D.A.G., 2012. Investigating the Fate and Transport Behavior of Cadmium Selenide Quantum Dots and Transition Metal Oxide Nanoparticles in Aquatic and Soil Environments. State University of New York at Buffalo.
Nga, P.T., Chinh, V.D., Hanh, V.T.H., Nghia, N.X., Dzung, P.T., Barthou, C., Benalloul, P., Laverdant, J., Maitre, A., 2011. Optical properties of normal and 'giant' multishell CdSe quantum dots for potential application in material science. International Journal of Nanotechnology 8, 347–359.
Pechstedt, K., Whittle, T., Baumberg, J., Melvin, T., 2010. Photoluminescence of colloidal CdSe/ZnS quantum dots: the critical effect of water molecules. Journal of Physical Chemistry C 114, 12069–12077.
Petosa, A.R., Jaisi, D.P., Quevedo, I.R., Elimelech, M., Tufenkji, N., 2010. Aggregation and deposition of engineered nanomaterials in aquatic environments: role of physicochemical interactions. Environmental Science & Technology 44, 6532–6549.
Pinheiro, J.P., Mota, A.M., Gonçalves, M.L.S., 1994. Complexation study of humic acids with cadmium (II) and lead (II). Analytica chimica acta 284, 525–537.
Schmidt, J., Vogelsberger, W., 2006. Dissolution kinetics of titanium dioxide nanoparticles: the observation of an unusual kinetic size effect. Journal of Physical Chemistry 110, 3955–3963.
Slaveykova, V.I., Startchev, K., 2009. Effect of natural organic matter and green microalga on carboxyl-polyethylene glycol coated CdSe/ZnS quantum dots stability and transformations under freshwater conditions. Environmental Pollution 157, 3445–3450.
Slaveykova, V.I., Startchev, K., Roberts, J., 2009. Amine- and carboxyl- quantum dots affect membrane integrity of bacterium *Cupriavidus metallidurans* CH34. Environmental Science & Technology 43, 5117–5122.
Sutherland, M.W., Learmonth, B.A., 1997. The tetrazolium dyes MTS and XTT provide new quantitative assays for superoxide and superoxide dismutase. Free Radical Research 27, 283–289.
Takeno, N., 2005. Atlas of Eh-pH diagrams. Geological Survey of Japan Open File Report, 1–287.
van Sark, W.G., Frederix, P.L.T.M., Van den Heuvel, D.J., Gerritsen, H.C., Bol, A.A., van Lingen, J.N.J., de Mello Donega, C., Meijerink, A., 2001. Photooxidation and photobleaching of single CdSe/ZnS quantum dots probed by room-temperature time-resolved spectroscopy. Journal of Physical Chemistry B 105, 8281–8284.
Vione, D., Feitosa-Felizzola, J., Minero, C., Chiron, S., 2009. Phototransformation of selected human-used macrolides in surface water: kinetics, model predictions and degradation pathways. Water Research 43, 1959–1967.
Walther, C., Meyer, K., Rennert, R., Neundorf, I., 2008. Quantum dot-carrier peptide conjugates suitable for imaging and delivery applications. Bioconjugate Chemistry 19, 2346–2356.
Wang, Q., Fang, T., Liu, P., Min, X., Li, X., 2011. Study of the bioeffects of CdTe quantum dots on *Escherichia coli* cells. Journal of Colloid and Interface Science 363, 476–480.
Yang, D., Rochette, J., Sacher, E., 2005. Spectroscopic evidence for $\pi-\pi$ interaction between poly (diallyl dimethylammonium) chloride and multiwalled carbon nanotubes. Journal of Physical Chemistry B 109, 4481–4484.
Zhang, C.Y., Hu, J., 2010. Single quantum dot-based nanosensor for multiple DNA detection. Analytical Chemistry 82, 1921–1927.
Zhang, C.Y., Yeh, H.C., Kuroki, M.T., Wang, T.H., 2005. Single-quantum-dot-based DNA nanosensor. Nature Material 4, 826–831.
Zhang, W., Yao, Y., Chen, Y.S., 2011a. Imaging and quantifying the morphology and nanoelectrical properties of quantum dot nanoparticles interacting with DNA. Journal of Physical Chemistry C 115, 599–606.
Zhang, W., Yao, Y., Sullivan, N., Chen, Y.S., 2011b. Modeling the primary size effects of citrate-coated silver nanoparticles on their ion release kinetics. Environmental Science & Technology 45, 4422–4428.
Zhang, W., Yao, Y., Li, K.G., Huang, Y., Chen, Y.S., 2011c. Influence of dissolved oxygen on aggregation kinetics of citrate-coated silver nanoparticles. Environmental Pollution. doi:10.1016/j.envpol.2011.1007.1013.
Zhang, Y., Chen, Y.S., Westerhoff, P., Crittenden, J.C., 2007. Stability and removal of water soluble CdTe quantum dots in water. Environmental Science & Technology 42, 321–325.
Zimnitsky, D., Jiang, C., Xu, J., Lin, Z., Zhang, L., Tsukruk, V.V., 2007. Photoluminescence of a freely suspended monolayer of quantum dots encapsulated into layer-by-layer films. Langmuir 23, 10176–10183.
Zook, J.M., Long, S.E., Cleveland, D., Geronimo, C.L.A., MacCuspie, R.I., 2011. Measuring silver nanoparticle dissolution in complex biological and environmental matrices using UV-visible absorbance. Analytical and Bioanalytical Chemistry. doi:10.1007/s00216-00011-05266-y.